17th Australasian Fluid Mechanics Conference
Auckland, New Zealand
5-9 December 2010

Flow around a square cylinder with a detached downstream flat plate at a low Reynolds number

Mohamed Sukri Mat Ali[1], Con J. Doolan[1] and Vincent Wheatley[2]

[1]School of Mechanical Engineering
The University of Adelaide, Adelaide, South Australia 5005, Australia

[2]School of Mechanical and Mining Engineering
The University of Queensland, Brisbane, Queensland 4072, Australia

Abstract

This paper investigates the interaction of a square cylinder wake with a detached flat plate of length equal to one cylinder height (D) at various downstream locations (G). Two modes of wake-plate interaction are observed from this study. For short gaps ($G \lesssim 2D$), a shear layer-plate interaction is observed, where the first flow regime is generated. In this regime, the shear layers roll up downstream of the plate. The optimal location of the plate is found at $G \sim 2D$ for maximum reductions in fundamental vortex shedding frequency, root mean square lift and mean drag of the cylinder. A sudden jump in Strouhal number is observed between $2D \lesssim G \lesssim 2.5D$, which suggests a transition into a new mode of wake-plate interaction. For long gaps ($2.5D \lesssim G \lesssim 5D$), a vortex-plate interaction is observed, where the second flow regime is generated. In this regime, the shear layers roll up within the gap, and the flow structure at near to the cylinder is almost unchanged with the gap.

Introduction

Bluff bodies are known for generating many flow-induced problems (e.g.; high pressure drag, unsteady forces, vibrations and aerodynamic noise). This condition is mainly associated with the periodic shedding of rolled up shear layers that originated from flow separations. Therefore, it is important to have an efficient means of flow control for the bluff bodies, so the flow-induced problems can be reduced or totally eliminated.

Wake interference is one of the effective passive flow controls for bluff bodies. Bluff bodies in a tandem arrangement is an example. The key parameter concerned for this case is the separation distance (G) between the bodies, since the flow properties may encounter a sudden change at a certain critical gap (G_c) [2, 3, 12, 15, 19].

Wake interference can also be obtained using a thin flat plate. The earliest and most extensive studies relate to a circular cylinder bluff body [9, 10, 14, 17]. These studies found that G_c is strongly related to the length of vortex formation completion. Therefore, other bluff geometries may have different values of G_c, and it is important to identify these values for the effectiveness of flow control.

The only available related study for the case of other than circular shape to investigate the effect of plate gap and to quantify the value of G_c is Farhadi et al. [8]. They numerically investigated a semi-circular cylinder with a downstream plate of chord length one cylinder diameter at $Re = 100$ to 500. They found that the critical gap for this configuration was $G_{c_{sc}} \sim 4.6D$, larger than for a circular cylinder ($G_{c_c} = 2.6D$) obtained by Hwang et al. [10] of the same Reynolds number ($Re = 100$).

The understanding of the flow structure variations with gap is also important for the effectiveness of sound reduction. For example, a preliminary study by Doolan [6] suggested that a detached flat plate can be used as a sound cancellation mechanism. Based on Curle's theory [5], Doolan theoretically showed that a total sound cancellation is possible when the lift force between the two bodies are similar but out of phase. However, the flow simulation showed [7] that it was very difficult to achieve this condition. This was because the inclusion of the plate in the wake of the cylinder introduced a strong hydrodynamic interaction between them.

The aims of this study are to inspect in detail the variations in flow structure for a square cylinder with a downstream detached flat plate, and to identify the critical gap of this configuration. To achive this, the separation distance between the cylinder and the plate is varied systematically, so any distinctive flow regimes and also its critical gap could be identified. This paper is organized as follows. After the introduction, test cases and the numerical simulations are described. Then, distinctive flow properties of the identified flow regimes are explained and the critical gap is quantified. The paper is concluded in the last section.

Test cases and numerical simulations

The test case under investigation is a rigid square cylinder of side length D immersed in a steady freestream velocity (U_∞) with a Reynolds number based on cylinder height of $Re = U_\infty D/\nu = 150$. This condition is called the unmodified condition. Then, a rigid thin flat plate is located downstream along the centerline of the cylinder. The chord length of the plate is the same as the side length of the cylinder ($L = D$). The separation distance (G), is measured from the rear surface of the cylinder to the leading edge of the plate, and is varied from $G = 0$ (attached plate) to $5D$, and the thickness of the splitter plate is fixed to $h = 0.02D$. Figure 1 shows a schematic diagram of the test case.

The primitive variables of the flow fields are calculated numerically based on the two-dimensional incompressible Navier-Stokes equations. The OpenFOAM [18] numerical simulation system is used to solve these governing equations. The 2nd-order backward scheme [11] is used for temporal discretisation, the convection term is discretised using the 3rd-order QUICK scheme [13] and 2nd-order unbounded Gauss linear differenc-

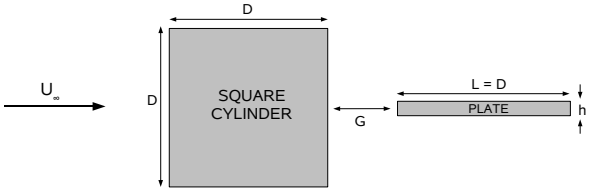

Figure 1: Sketch of the test case and annotations.

ing scheme is used for the viscous term. The time step for pressure, convection and diffusion terms is set at $\Delta t U_\infty / D = 0.002$ with the requirement to keep the CFL number [4] below 0.5. All of the analyses are made from a set of sampling data of at least 10 vortex shedding periods after a statistically stationary flow condition is achieved.

The computational domain of the finest grid solution (case E) of Ali et. al. [1] is used for the unmodified square cylinder case of this current study. For cases of a square cylinder with a detached plate, the grid domain is extended downstream according to the corresponding gap, so the streamwise distance between the trailing edge and the downstream computational domain is always $20D$. The plate has 204 cells along the edges. Within the gap, a uniform mesh with cells being spaced equally at 100 cells for every cylinder side length (D) is constructed, to maintain the same grid resolution in the near wake region as the unmodified case. Other grid parameters are set the same as the unmodified square cylinder case.

Results

Two distinct flow regimes are observed when the gap between the cylinder and the plate is varied from $G = 0$ (attached plate) to $5D$. Figure 2 shows a comparison of instanteneous streamwise vorticity contours between regime I, represented by $G = 2D$, and regime II, represented by $G = 2.5D$. The first regime is for $G \lesssim 2D$. In this regime, the separated shear layers from the upstream corners interact with the plate (named the shear layer-plate interaction) before they roll up forming large scale vortices. This is similar to the numerical study by Doolan [7], and detailed explanations about the vortex formation process can be found from that study. The current study provides additional information particularly concerned with the effect of the gap length. When the gap is increased, the interaction between the shear layers and the plate becomes more intense, consequently, the secondary vortices grow along the edges of the plate. Then, the secondary vortices slowly merge with the growing primary vortices of the same sign of rotation.

The second identified flow regime is for gaps in the range of $2.5D \lesssim G \lesssim 5D$. In this regime, the shear layers roll up within the gap. Near the base of the cylinder, a well organized flow structure is observed, and it is almost similar to the case of unmodified square cylinder. This is because the shear layers roll up almost independently within the gap. It is also observed that there is an incipient small scale vortex engulfing the rear surface of the cylinder due to the face-wide vertical flow induced by the shear layers. The flow field near the plate is more complex. This is due to the interaction between the fully grown vortex and the plate (named the vortex-plate interaction). The plate trims the oncoming vortex into two parts. One part of the trimmed vortex is being convected downstream to form a von Kármán street vortex. The other part of the trimmed vortex is relatively small, and is rapidly diffused.

The flow regimes identified earlier can also be observed clearly from the time-avergared flow properties. Figure 3 shows a comparison of time-averaged streamwise normal stress (U_{xx}/U_∞^2) contours between regime I (i.e; $G = 2D$) and regime II (i.e; $G = 2.5D$). For regime I, a pair of high level of U_{xx} concentrations is observed. This is attributed to the completion of the vortex formation process. For regime II, two pairs of U_{xx} concentrations are observed. The first pair of U_{xx} concentrations is located before the plate. The other pair of U_{xx} concentrations is located near the trailing edge of the plate, and it is generated by the vortex-plate interaction that amplifies the velocity fluctuations. The figure also shows the recirculation region (broken line) for the respective regime. For regime I, the plate is in-

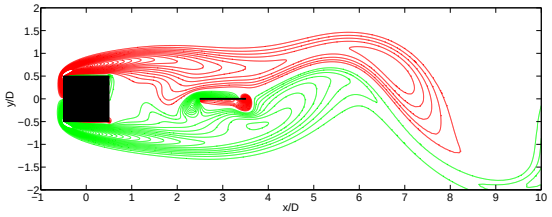

(a) regime I, i.e; $G = 2D$

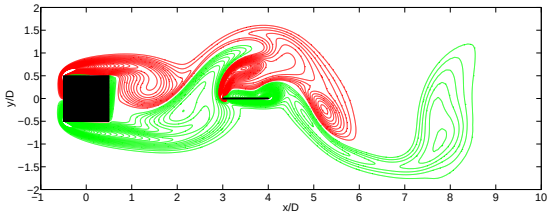

(b) regime II, i.e; $G = 2.5D$

Figure 2: Spanwise vorticity contours at a time of maximum lift coefficient about the cylinder, coloured by direction of rotation, red: clockwise direction, $-4.0 \leq \frac{\Omega D}{U_\infty} \leq -0.3$; and green: anticlockwise, $0.3 \leq \frac{\Omega D}{U_\infty} \leq 4.0$ of plate length of $L/D = 1$.

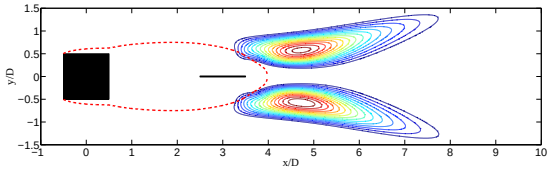

(a) regime I, i.e; $G = 2D$

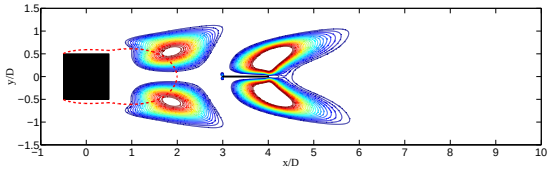

(b) regime II, i.e; $G = 2.5D$

Figure 3: Contours of time-averaged streamwise normal stress ($\frac{U_{xx}}{U_\infty^2}$). The contour levels are from 0.04 to 0.15 with a constant increment of 0.005. The contours are superimposed with a red dashed line indicating the recirculation zone.

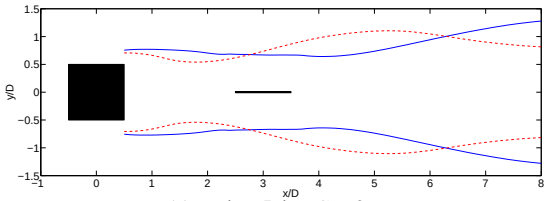

(a) regime I, i.e; $G = 2D$

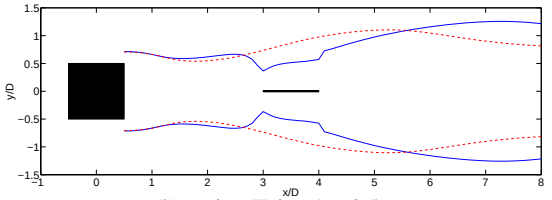

(b) regime II, i.e; $G = 2.5D$

Figure 4: Comparison of half-width wake thickness ($y_{1/2}/D$) between $G = 2D$ and $G = 2.5D$. The dashed lines are $y_{1/2}/D$ for the unmodified square cylinder.

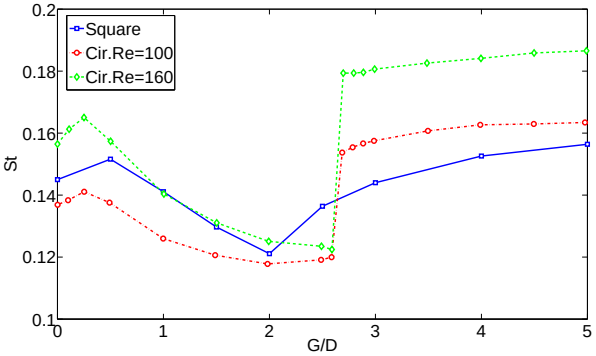

Figure 5: Variation of non-dimensional vortex shedding frequency (St) with G/D. -□-; square cylinder of current study, and -◯-; circular cylinder at $Re = 100$, and -◇- circular cylinder at $Re = 160$ by numerical study of [10].

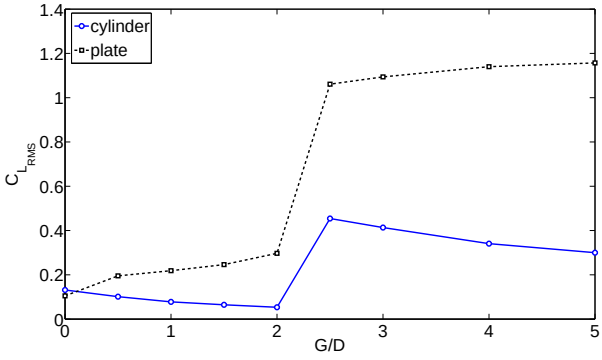

Figure 6: Variation of root mean square lift coefficient ($C_{L_{RMS}}$) with G/D.

side the bubble, and the length of the bubble increases with gap. But for regime II, the plate is outside the bubble and the size is almost constant with the variation of gaps. Thus, for the the second flow regime, the near wake of the cylinder is not affected significantly by the plate and the flow structure is similar to the case of an isolated bluff body.

Figure 4 shows a comparison of half-width wake thickness ($y_{1/2}/D$) for regime I (i.e; $G = 2D$) and regime II (i.e; $G = 2.5D$). The half-width wake thickness is defined as [16];

$$U_s = U_\infty - \overline{u}(x, y_{(|\overline{u}|_{max})}) \quad (1)$$

$$\overline{u}(x, \pm y_{1/2}) = U_\infty - \frac{1}{2}U_s \quad (2)$$

where $|\overline{u}|_{max}$, U_∞ and $\overline{u}$ are maximum defect velocity, free stream velocity and time-averaged streamwise velocity, respectively. A well defined minimum value of $y_{1/2}/D$ is observed for regime I, but not for regime II. For regime I, the completion of the vortex formation creates a low pressure region that consequently squeezes the wake of the cylinder. However, for regime II, in addition to the necking point due to the vortex formation process, there are discontinuities in the lines of $y_{1/2}/D$ that occurs at both ends of the plate. This condition is due to the strong interaction between the vortex and the plate.

Figure 5 shows the variations of Strouhal number ($St = f\frac{D}{U_\infty}$, where f is the vortex shedding frequency, D and U_∞ are the side length of the cylinder and the free stream velocity, respectively) with the gap. When the plate is detached from the cylinder to $G = 0.5D$, a sudden increase in Strouhal number is detected. This is due to the existence of two secondary vortices (instead of one for the case of attached plate), each at the ends of the plate, that brings additional perturbation to the shear layer's instability.

For the gaps in the range of $0.5D \lesssim G \lesssim 2D$, the plate pushes the vortex formation completion further downstream when the gap is increased. Consequently, the Strouhal number decreases with the gap. Then, beyond $G \sim 2D$ the shear layers have reached their limit, where they cannot be convected further downstream before rolling up. Thus, the shear layers become unstable and the vortex formation occurs within the gap. This condition makes the Strouhal number increase significantly. For the second regime, the Strouhal number slowly increases. The reason for this is not yet understood at this stage of study, but it is probably due to the minimum wake width of the cylinder that becomes narrower when the gap is increased.

Figure 5 also compares the variations of Strouhal number for the case of a circular cylinder with detached plate from the numerical study of ref. [10]. The critical gap for a circular cylinder is $G_{c_{circular}} \sim 2.6D$, and for the square cylinder of the current study is smaller than that ($2D \lesssim G_{c_{square}} \lesssim 2.5D$, as further study is needed to refine the transition region). The trend in the variation of St with G is almost similar for circular and square cylinder cases, except in the second flow regime, where for the circular cylinder case, there is a jump of St in the transition regime before it becomes almost constant.

Figure 6 shows the variations of root mean square lift coefficient fluctuations with G/D for the cylinder ($C_{L_{RMS_c}}$) and for the plate ($C_{L_{RMS_p}}$). For the first flow regime ($G \lesssim 2D$), the magnitude of $C_{L_{RMS_c}}$ decreases with gap length. This is attributed to the generation of less compact vortices near of the cylinder, as the shear layers roll up further downstream, they provide more opportunity for the vortex diffusion. However, the magnitude of $C_{L_{RMS_p}}$ increases with the gap, as the plate moves closer to the point of vortex formation completion, at which the strength of the vortex is the strongest.

A sudden jump in $C_{L_{RMS_c}}$ and $C_{L_{RMS_p}}$ is observed in the transition regime ($2D \lesssim G \lesssim 2.5D$), and the magnitude of $C_{L_{RMS_c}}$ is far greater than for the unmodified square cylinder ($C_{L_{RMS_0}} = 0.28$) [1]. This is because the vortex-plate interaction generates a large surface pressure variation in the vicinity of the plate. This condition amplifies the surface pressure on the cylinder. But the effect is weakened when the plate moves further downstream. Thus, the magnitude of $C_{L_{RMS_c}}$ decreases with the gap. For the magnitude of $C_{L_{RMS_p}}$, the changes are very small, and almost identical at long gaps, as the vortices are well formed and organized before they hit the plate.

Figure 7 shows the variation of mean drag coefficient for the cylinder ($C_{D_{mean_c}}$) and for the plate ($C_{D_{mean_p}}$) with the effect of gap. For the first flow regime, as the plate is inside the recirculation region, the plate experiences a thrust (negative viscous drag). The thrust increases as the plate moves closer to the saddle point of the recirculation region. However, a non-monotonic change is observed for the mean drag of the cylinder. The magnitude of $C_{D_{mean_c}}$ increases when the plate is first detached from the cylinder (i.e.;from $G = 0$ to $0.5D$). This is because the gap provide a space for the fluid to be entrained across the wake centerline, that decreases the pressure on the base of the cylinder. But, then it gradually decreases when the gap is further increased. This condition is related to vortex formation, where the vortex forms further downstream as the gap is increased, hence, more pressure recovery can be obtained at the base of the cylinder.

A sudden increase in the mean drag for both bodies is observed

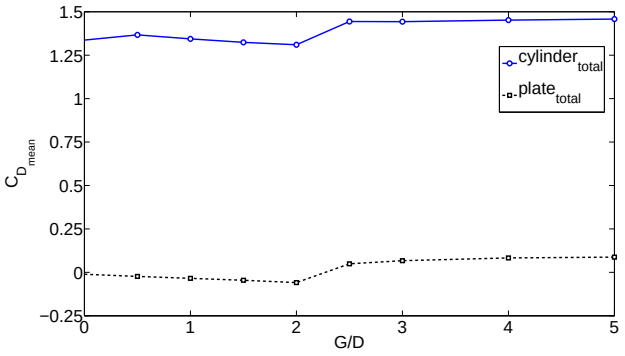

Figure 7: Variation of mean drag coefficient fluctuations with G/D

in the transition regime. Then, for the second flow regime, the variation of mean drag is almost constant, and the plate experiences a positive drag, as the plate is now located outside of the recirculation region.

Conclusions

The flow around a square cylinder with a downstream plate at various gap lengths (G) has been investigated numerically at $Re = 150$. Two distinctive flow regimes are identified according to the gap length. For the first flow regime ($G \lesssim 2D$), the shear layers roll up after the gap, but this occurs closer to the gap as the gap is increased. A significant increase in aerodynamic forces is observed in the transition into a new regime, and the critical gap lies between $2D \lesssim G_c \lesssim 2.5D$. A further study is required to identify accurately this critical gap, by refining the transition regime. For the second flow regime ($2.5D \lesssim G \lesssim 5D$), the shear layers roll up within the gap and the flow structure near the cylinder is almost constant with the variation of the gap.

Acknowledgements

The authors would like to acknowledge eResearchSA for the use of their supercomputing facilities. The first author also would like to acknowledge Universiti Teknologi Malaysia for the receipt of Ph.D scholarship.

References

[1] Ali, M. S. M., Doolan, C. J. and Wheatley, V., Grid convergence study for a two-dimensional simulation of flow around a square cylinder at a low reynolds number, in *Seventh International Conference on CFD in The Minerals and Process Industries*, CSIRO, Melbourne, Australia, 2009.

[2] Bull, M. K., Blazewicz, A. M., Pickles, J. M. and Bies, D. A., Interaction between a vortex wake and an immersed rectangular plate, *Experimental Thermal and Fluid Science*, **12**, 1996, 209 – 220.

[3] Carmo, B. S., Meneghini, J. R. and Sherwin, S. J., Secondary instabilities in the flow around two circular cylinders in tandem, *Journal of Fluid Mechanics*, **644**, 2010, 395–431.

[4] Courant, R., Friedrichs, K. and Lewy, H., On the partial difference equations of mathematical physics, *IBM J. Res. Dev.*, **11**, 1967, 215–234.

[5] Curle, N., The influence of solid boundaries upon aerodynamic sound, *Proceedings of the Royal Society of London. Series A, Mathematical and Physical Sciences*, **231**, 1955, 505–514.

[6] Doolan, C. J., Bluff body noise reduction using aerodynamic interference, in *Australian Institute of Physics (AIP), 18th National Congress*, Adelaide, South Australia, 2008.

[7] Doolan, C. J., Flat-plate interaction with the near wake of a square cylinder, *AIAA Journal*, **47**, 2009, 475–478.

[8] Farhadi, M., Sedighi, K. and Fattahi, E., Effect of a splitter plate on flow over a semi-circular cylinder, *Proceedings of the Institution of Mechanical Engineers, Part G: Journal of Aerospace Engineering*, **224**, 2010, 321–330.

[9] Hwang, J.-Y. and Yang, K.-S., Drag reduction on a circular cylinder using dual detached splitter plates, *Journal of Wind Engineering and Industrial Aerodynamics*, **95**, 2007, 551 – 564.

[10] Hwang, J.-Y., Yang, K.-S. and Sun, S.-H., Reduction of flow-induced forces on a circular cylinder using a detached splitter plate, *Physics of Fluids*, **15**, 2003, 2433–2436.

[11] Jasak, H., *Error analysis and estimation for the finite volume method with applications to fluid flows*, Ph.D. thesis, Department of Mechanical Engineering, Imperial College of Science, Technology and Medicine, 1996.

[12] Leclercq, D. and Doolan, C., The interaction of a bluff body with a vortex wake, *Journal of Fluids and Structures*, **25**, 2009, 867 – 888.

[13] Leonard, B. P., A stable and accurate convective modelling procedure based on quadratic upstream interpolation, *Computer Methods in Applied Mechanics and Engineering*, **19**, 1979, 59 – 98.

[14] Ozono, S., Flow control of vortex shedding by a short splitter plate asymmetrically arranged downstream of a cylinder, *Physics of Fluids*, **11**, 1999, 2928–2934.

[15] Papaioannou, G. V., Yue, D. K. P., Triantafyllou, M. S. and Karniadakis, G. E., Three-dimensionality effects in flow around two tandem cylinders, *Journal of Fluid Mechanics*, **558**, 2006, 387–413.

[16] Pope, S. B., *Turbulent Flows*, Cambridge University Press, 2000.

[17] Roshko, A., On the drag and shedding frequency of two-dimensional bluff bodies, *NACA Technical Note*, **TN 3169**.

[18] Weller, H. G., Tabor, G., Jasak, H. and Fureby, C., A tensorial approach to computational continuum mechanics using object-oriented techniques, *Computer in physics*, **12**, 1998, 620–631.

[19] Zdravkovich, M. M., The effects of interference between circular cylinders in cross flow, *Journal of fluids and structures*, **1**, 1987, 239–261.